Athanasiadou, G., Nix, A. R., & McGeehan, J. P. (1998). Investigation into the sensitivity of a microcellular ray-tracing model and comparison of the predictions with narrowband measurements. In Unknown. (Vol. 2, pp. 870 - 874). Institute of Electrical and Electronics Engineers (IEEE). 10.1109/VETEC.1998.683706

Investigation into the sensitivity of a microcellular ray-tracing model and comparison of the predictions with narrowband measurements

G.E. Athanasiadou, A.R. Nix, J.P. McGeehan

Centre for Communications Research, University of Bristol,
Merchant & Venturers Building, Woodland Road, Bristol BS8 1UB, UK.
Fax: +44 (0)117 9545206, Tel. +44 (0) 117 9545203, E-mail: G.Athanasiadou@bristol.ac.uk

Abstract: **In this paper the sensitivity of a 3D image-based ray tracing model for microcellular environments [1-2] is investigated. The variation of the received power is examined for different ray permutations and wall characteristics. The predictions of the different configurations are compared with narrowband measurements performed in a typical urban area.**

The analysis illustrates that with 5 orders of reflection and 1 order of diffraction the model produces reliable results. It is also shown that good agreement with measured results can be obtained for wall conductivity in the order of 10^{-3}S/m and values of relative permitivity around 5.

I. INTRODUCTION

During the last decade ray tracing has emerged as the dominant technique for small cell propagation modelling. Naturally, two of the most critical issues related to all propagation models are accuracy and sensitivity of their predictions [3-5]. In [1-2] the model employed here was presented, in [3] its accuracy was investigated and in this paper the sensitivity of the power predictions to various input parameters is examined.

The ray tracing algorithm is based on the theory of images. The model allows the rapid generation of complex channel impulse response characteristics and, with sufficient memory, can evaluate scenarios incorporating many thousands of objects. In this model a hybrid technique is applied where the object database is held in two dimensions but the ray-tracing engine operates in three dimensions. The base station and the mobiles are assumed to remain below roof top height and based on this assumption, the buildings are modelled as infinitely tall. However, the antenna heights are specified and the ground is also considered. The rays are traced in 3D space and all reflections, transmissions and diffractions are computed using 3-D vector mathematics. This hybrid analysis allows factors such as polarisation and 3D antenna patterns to be fully considered. For a more detailed description of the model, see references [1-2].

II. MEASUREMENT SET UP

The power predictions of the model are compared with narrowband measurements taken in a typical urban area, in central Bristol, UK. The field trials were performed under the British Telecom VURI project [6]. The measurement site (Figure 1) was a well developed urban area with multi-storey buildings. The transmitting antenna was on a mast at a height of 5m above ground level. The frequency was 1.823GHz and the transmitted power was 30dBm (including the cable and antenna losses). The receiver was at a height of 1.57m, mounted on a trolley which was slowly and carefully moved along the predefined route shown in Figure 1. Both antennas were typical half wavelength vertically polarised dipoles, below the roof height of adjacent buildings. The test route includes LOS, NLOS and also deep shadow areas where energy can reach the receiver only through multiple reflected and diffracted rays.

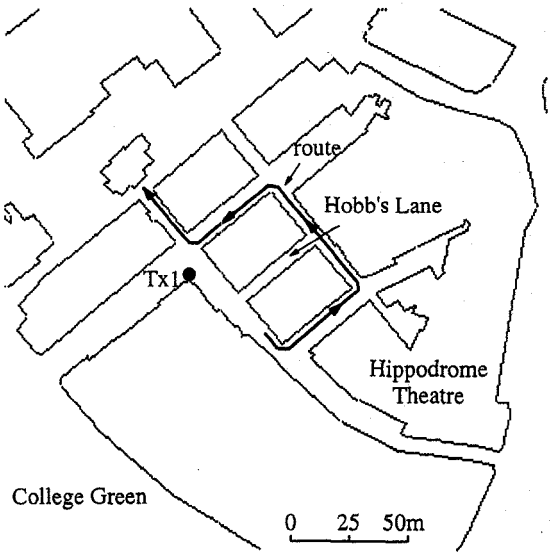

Figure 1: Microcellular map of the measurement area.

The narrowband receiver used for the measurements recorded field strength against distance from the starting point, with a spatial sampling rate of 4cm. The fast fading of each measurement was extracted with a rectangular sliding window averaging process. A 10 wavelength window was chosen (equivalent to 1.67m), so that the measurements maintain their site specific information as much as possible. Six measurement runs were performed along the same route and with the same configuration. For more representative results (in order to remove localised temporal effects), the slow fading envelopes were averaged to produce a mean envelope.

0-7803-4320-4/98/$5.00 © 1998 IEEE

III. Model Set up and Comparison Between Measurements and Predictions

The Bristol building data was extracted from the UK Ordnance survey 'Landline' database. The map was then pre-processed to remove any redundant information and diffraction corners were automatically added. The simulated area (part of which is shown in Figure 1) is approximately 500x500m^2 and contains 438 walls. For the results shown below, the permitivity of the walls is ε_r=5 and the conductivity σ=0.005 Sm^{-1} [7-8], unless it is otherwise stated. The walls were assumed smooth and to have a thickness of 0.6m. Unlike the field trials, the space resolution between the prediction points was 0.5m. This is because the predicted received power which is produced as the sum of the power of the rays reaching the receiver, is inherently time averaged and no further action is needed to remove the fast fading.

Figure 2 depicts the mean measured envelope, along with the predictions when rays with up to 7 orders of reflection and 2 orders of diffraction are considered in the model. The simulation results agree well with the measurement trend throughout the route, remaining within a few dB from the mean measurement for the majority of the receiver positions. The mean difference between the predictions and the measurements is 0.97dB with an RMS error of 3.4dB (all errors are calculated with both measurements and predictions in the logarithmic scale).

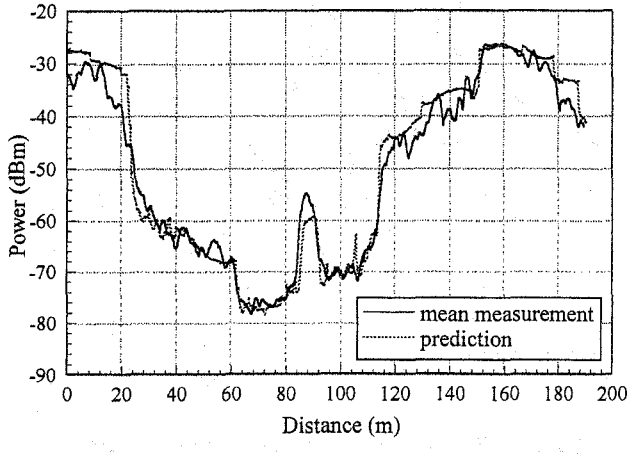

Figure 2: Model's prediction against mean measurement.

IV. Investigation into the Sensitivity of the Microcellular Ray Tracing Model

In this section the sensitivity of the microcellular propagation model to various simulation parameters is investigated. The variation of the received power is examined for different ray permutations and wall characteristics. Taking advantage of the narrowband measurements presented in the previous section, the power predictions are also compared with the measured results.

IV.a Sensitivity to the Maximum Permitted Ray Interactions with the Environment.

The basic propagation mechanisms used by the model are specular reflection, corner diffraction and wall transmission. In this section, the sensitivity of the microcellular model to the maximum permitted orders of reflection and diffraction is investigated. Although wall transmitted rays are also supported, this propagation mechanism is generally ignored for outdoor microcellular studies and only used in order to predict outdoor-to-indoor and indoor-to-outdoor coverage.

Sensitivity to the maximum permitted order of reflection

As depicted in Figure 3, results are compared for 3, 5, 7 and 9 orders of reflection and 1 order of diffraction. At LOS areas, the signal level is the same for all the above ray permutations. At these areas the received power is determined by a few dominant rays, the direct together with some strong rays with only one or two orders of reflection. As the receiver enters into NLOS areas where the previously dominant rays cannot reach, higher orders of reflections are needed in order to obtain accurate power predictions. The more shadowed the NLOS area, the more reflections are required for the predictions to reach their final values. At the deep shadow areas between the second and third corner of the route (between ~62m and 115m in Figure 3), the difference between the predictions with the highest (9) and the lowest (3) permitted orders of reflection is 9.6dB on average, while at some points, it is as high as 21.5dB. Along this section of the route, the predictions improve dramatically when the number of reflections increases from 3 to 5.

Table 1 depicts the error statistics of the results with the above model configurations in comparison with the mean measurement along the same route. The RMS error decreases with the increasing number of reflections. With 5 or more reflections, in conjunction with 1 diffraction, the RMS error is below 3.9dB, while the mean error is less than 0.9dB.

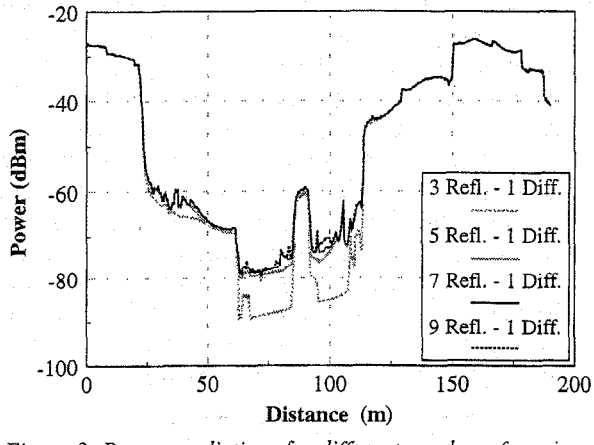

Figure 3: Power predictions for different number of maximum allowed reflections.

	Mean error (dB)	RMS error (dB)
3 refl. - 1 diff.	-2.2592	7.1741
5 refl. - 1 diff.	0.3214	3.8421
7 refl. - 1 diff.	0.7345	3.5416
9 refl. - 1 diff.	0.8553	3.4817

Table 1: Mean and RMS errors with respect to the measured results.

	Mean error (dB)	RMS error (dB)
7 refl. - 0 diff.	-12.5290	27.9838
7 refl. - 1 diff.	0.7106	3.5355
7 refl. - 2 diff.	0.9703	3.4017
7 refl. - 3 diff.	0.9967	3.4095

Table 2: Mean and RMS errors with respect to the measured results.

Sensitivity to the maximum permitted order of diffraction

The role of corner diffraction in the modelling of the outdoor environments is investigated here. Simulation results with 0, 1, 2 and 3 maximum orders of diffraction, together with 7 orders of reflection are compared with each other and with the narrowband measurements. As illustrated in Figure 4, diffraction is a very significant propagation mechanism for the study of outdoor scenarios. When no diffractions are considered, only the channel characteristics of the LOS areas can be predicted, while for long sections of the route no rays reach the receiver, even after 7 orders of reflection (e.g. between 65.5m and 79.5m). Moreover in areas where strong reflections exist, diffraction affects the predictions by making smoother the transition from LOS to NLOS areas and in and out of the illuminated areas of strong reflections (between ~115m and 150m and also from ~179m and onwards). However, rays with as many as 3 diffractions are far too attenuated to influence the model's predictions. The maximum difference between the power predictions with 3 and 1 orders of diffractions is 1.55dB. The RMS difference between the results with 3 orders and those with 1 and 2 is 0.50dB and 0.08dB respectively. As shown in Table 2, in comparison with the measurements, the errors for 1, 2 and 3 orders of diffraction are almost the same (in all three cases the mean and RMS errors are ~0.99dB and ~3.5dB, respectively).

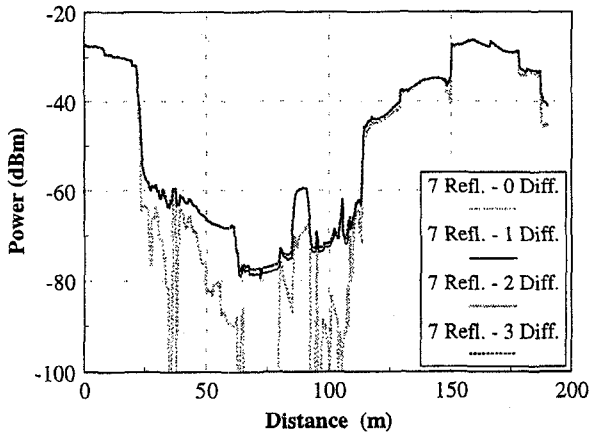

Figure 4: Power predictions for different orders of corner diffraction.

Number of traced rays

Figure 5 shows the number of rays detected by the model for different ray permutations and with power greater than a power threshold of -150dBm (user definable). This is only a subtotal of the actual number of the traced rays at each point, since valid rays with power less than the predefined power threshold, are not considered. As expected, more rays are traced by the model as the maximum permitted interactions with the environment rises. The mean number of rays increases from 122 to 1037 as the reflections rise from 3 to 9, with 1 order of diffraction. When 3, 5 and 7 orders of reflection and 1 diffraction are considered in the study, the rays found are 9.32%, 37.89% and 94.15%, respectively, of those traced when up to 9 reflections and 1 diffraction are permitted in the model.

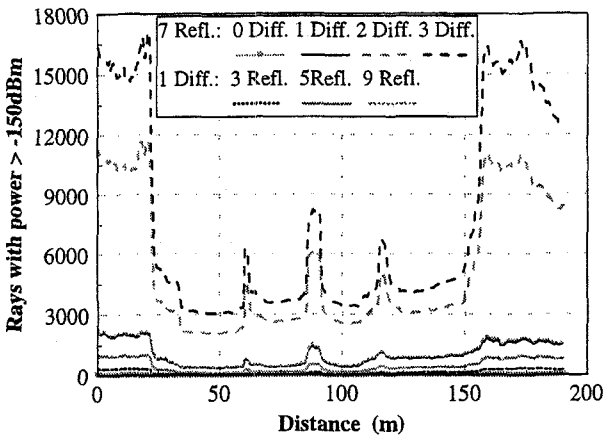

Figure 5: The number of traced rays (with power > -150dBm) for different ray permutations.

However, what is really striking is the complexity that each extra order of diffraction adds to the model. Each illuminated diffraction corner acts as a secondary source which launches rays in all directions. Moreover, each additional order of diffraction increases the flexibility of the rays and as a result, raises dramatically the total number of generated images and the traced rays at each receiving point. Hence, with up to 7 reflections and 0, 1, 2 and 3 orders of diffraction, the mean number of rays along the route is 15, 984, 5234 and 7534, respectively, while for the same interactions, the maximum number of rays is 52, 2302, 11756 and 17135, respectively. Most of these rays are very weak and do not contribute to the channel characterisation,

while the strong and most significant ones are only a small portion of the traced rays. Permitting up to 7 reflections and 1 diffraction, the number of rays found with power greater than -150dBm, together with the number of rays for which the power is inside a 30dB window from the strongest ray at that specific point, are depicted in Figure 6. There is obviously a disproportional relationship between these two numbers. In LOS areas where the model can trace many thousands of rays, only a few of them (less than 0.5%) are really important. As the mobile enters into NLOS areas where less powerful rays exist, the power levels fall and more rays are included in the 30dB window. In the best case, just 11.1% (340 rays) of the traced rays have power inside the 30dB window.

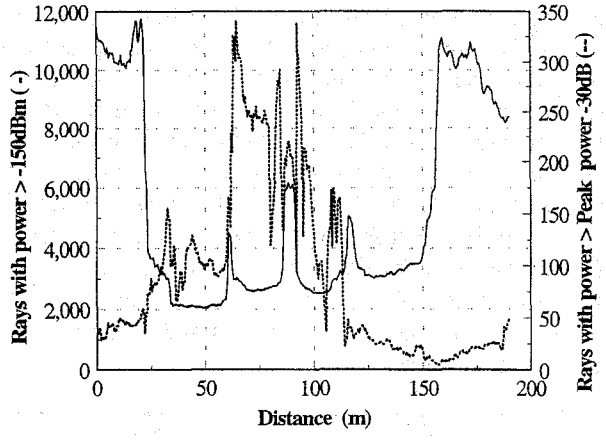

Figure 6: Total number of rays (considering 7 reflections and 2 diffractions) together with the number of rays inside a 30dB window from the strongest ray.

Although at each point only a few of the traced rays contribute to the channel characterisation, it is important that the model can handle a very large number of rays, in order to produce reliable results for complex environments, even in deep shadow areas away from the transmitter. The outdoor model investigated here is capable of handling a very large number of rays and supports the wideband, as well as the narrowband, characterisation of complex microcellular environments.

IV.b MODEL'S SENSITIVITY TO THE WALLS' CHARACTERISATION

In this section, the sensitivity of the power results to the walls' electrical characteristics is investigated. Each object in the building database is characterised by its conductivity (σ) and relative permitivity (ε_r). By changing one of the wall characteristics at a time, the sensitivity of the model to that parameter is evaluated. The results below are for 7 orders of reflection and 1 order of diffraction.

First, the behaviour of the model is examined as the values of conductivity range from 10^{-12}S/m to 10S/m while the relative permitivity of the walls is 5. As depicted in Figure 7, while the conductivity remains relatively low (10^{-12} - 0.0005S/m), the power predictions do not alter considerably. Indeed, the mean difference between the results with very low conductivity ($\sigma = 10^{-12}$S/m) and those with σ = 0.0005S/m is just 0.59dB with a standard deviation of 0.40dB, while their maximum difference along the route is 2.13dB. By further increasing the conductivity by one order of magnitude (σ = 0.005S/m), a considerable drop in the received signal levels appears in the results. The power decrease is 2.66dB on average, but at certain receiver positions it is as high as 10.56dB. As the walls become more conductive (σ = 10S/m), the channel characteristics change significantly. As expected, the received power increases dramatically (up to 38.16dB at certain points). As depicted in Table 3, the mean error with respect to the measurements varies from 5.2dB to 3.5dB and the RMS error from 3.9dB to 0.7dB as the conductivity values range from 10^{-12}S/m to 0.0005S/m.

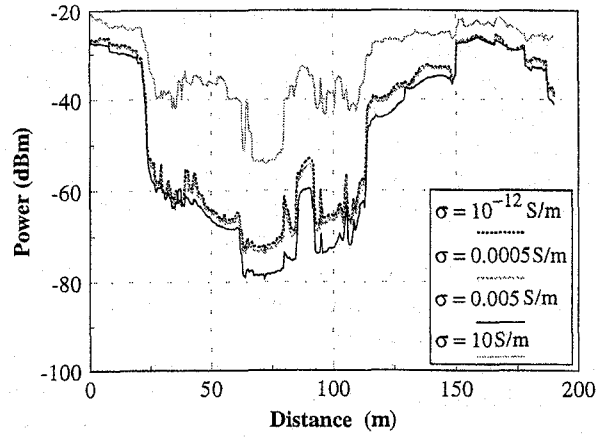

Figure 7:Power predictions for various values of wall conductivity.

	Mean error (dB)	RMS error (dB)
$\sigma = 10^{-12}$ S/m	3.9754	5.2514
$\sigma = 5*10^{-4}$ S/m	3.3787	4.7672
$\sigma = 5*10^{-3}$ S/m	0.7106	3.5355
σ = 10 S/m	18.5292	20.6463

Table 3: Mean and RMS errors with respect to the measured results.

Similar analysis is performed in order to examine the effect of the walls' relative permitivity on the predictions. For this study, the conductivity is 0.005S/m. The power predictions are examined for wall permitivity 3, 3.5, 5 and 7 (Figure 8). The predictions with permitivity 3.5 and 7 are relatively close to the evaluations for ε_r =5, with RMS errors of 2.3dB and 3.7dB, respectively, while the RMS error for ε_r = 3 is 5.45dB. Generally, as the value of permitivity rises, so does the received power as well. For the whole route, the mean power for permitivity 3, 3.5, 5 and 7 is -54.84dBm, -51.53dBm, -49.84dBm and -47.28dBm, respectively. Table

4 shows the error statistics of all the above predictions with respect to the measurements. The resulting RMS errors fluctuate as much as 3.2dB. The RMS errors of the evaluations with permitivity 3.5 and 5 are both less than 4dB (3.98dB and 3.53dB, respectively). The worst error in comparison with the measurements is 6.70dB and occurs for $\varepsilon_r = 3$.

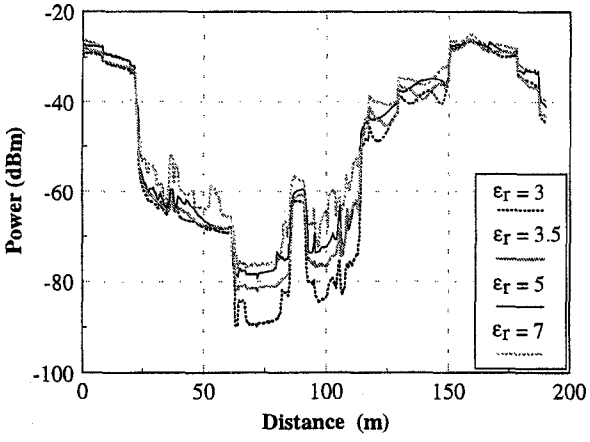

Figure 8: Power predictions for different values of wall permitivity.

	Mean error (dB)	RMS error (dB)
$\varepsilon_r = 3$	-3.2933	6.7026
$\varepsilon_r = 3.5$	-0.9848	3.9895
$\varepsilon_r = 5$	0.7106	3.5355
$\varepsilon_r = 7$	3.2746	4.5786

Table 4: Mean and RMS errors with respect to the measured results.

V. Discussion - Conclusions

In this paper the sensitivity of the 3D ray tracing microcellular model presented in [1-2], was investigated. The variation of the predictions was examined for different ray permutations and wall characteristics (conductivity, permitivity).

Ideally, for an outdoor environment to be modelled, a very large number of ray interactions with the environment should be considered. The sensitivity analysis of the model to the maximum permitted ray interactions illustrated that after a certain number of reflections and diffractions, the addition of extra orders did not affect the results, since at each point the predictions converged to a constant value. At LOS positions and in the regions where strong rays existed, a few orders of reflection were adequate to predict the received power. However, as the receiver moved into areas where only multi-reflected and diffracted rays could reach, more reflections and diffractions were needed in order to obtain reliable results. The great importance of diffraction in the outdoor environments was also illustrated since, despite the considerable complexity that diffraction adds to the model, without this propagation mechanism, the model could not give any predictions for the majority of the NLOS area. For up to 7 orders of reflection and 2 orders of diffraction the predictions were very close to the values of convergence. In this case, the RMS error with respect to the measurements was 3.4dB. If the run-time is important, 5 reflections with 1 diffraction appeared to be a reasonable compromise for a typical coverage study (RMS error = 3.8dB).

In order to analyse how the predictions of the model were affected by the values of conductivity and permitivity of the simulated walls, all the objects in the building database were characterised by the same set of values. By changing one of the wall characteristics at a time, the sensitivity of the model to that parameter was evaluated. It was shown that for the scenario under investigation (a typical urban environment in the centre of Bristol), good agreement with the measured power results (RMS error ~ 4dB) could be obtained for wall conductivity in the order of 10^{-3}S/m and values of relative permitivity around 5.

VI. Acknowledgements

The measurements and the sensitivity analysis shown in this paper were partly funded by British Telecom as part of the Virtual University Research Initiative (VURI) project. The authors would like to thank Dr G. Tsoulos for his helpful suggestions.

VII. References

[1] G.E.Athanasiadou, A.R.Nix, J.P.McGeehan, "A ray tracing algorithm for microcellular and indoor propagation modelling", *IEE ICAP '95*, pp. 2.231-2.235, Eindhoven Holland, 4-7 April 1995.

[2] G.E.Athanasiadou, A.R.Nix, J.P.McGeehan, "A ray tracing algorithm for microcellular wideband propagation modelling", *IEEE VTC '95*, pp. 261-265, Chicago USA, 25-28 July 1995.

[3] G.E.Athanasiadou, A.R.Nix, J.P.McGeehan, " Comparison of Predictions from a Ray Tracing Microcellular Model with Narrowband Measurements ", IEEE VTC '97, pp. 800-805, Phoenix USA, 4-7 May 1997.

[4] K. Rizk, J.-F. Wagen, F. Gardiol, 'Two-Dimensional Ray-Tracing Modelling for Propagation Prediction in Microcellular Environments', *IEEE Transactions on Vehicular Technology*, Vol. 46, No. 2, pp. 508-518, May 1997.

[5] S.S. Wang, J.D. Reed, 'Analysis of Parameter Sensitivity in a Ray-Tracing Propagation Environment', *IEEE VTC '97*, pp. 805-809, Phoenix, USA, 4-7 May 1997.

[6] S.A.Meade, A.R.Nix, M.A.Beach, "Summary of the Processing of the Narrowband Measurement Data for Microcells", University of Bristol, August 1996, Technical Report for the BT VURI project.

[7] Von Hippel, *Dielectric Materials and Applications*, The Technology Press of MIT and John Wiley & sons, Inc., New York, NY, 1954.

[8] *American Institute of Physics Handbook*, 3rd edition, McGraw-Hill, New York, NY, 1972.